SUPPLEMENTARY DATA

Supplementary information

Drugs

Rats received an intracerebroventricular (ICV) administration of 5 μL of vehicle or MCH (20 μg; Bachem, Bubendorf, Switzerland). For the inhibition of SIRT1, we used a potent specific inhibitor of SIRT1: Ex527 (10 μg in a total volume of 5 μL; Tocris Bioscience, St. Louis, MO). Mice were treated icv with MCH sense or MCH-ASO phosphorthioate-modified oligonucleotides. MCH sense and MCH-ASO were diluted in TE buffer (10 mM Tris–HCl, 1 mM EDTA) and injected at the beginning of the light cycle in a total volume of 2 μl per mouse. Phosphorthioate modified oligonucleotides for MCH (sense, 5_-CCC TCA GTC TGG CTG-3_ and anti-sense, 5_-ACA GCC AGA CTG AGG- 3) were obtained from Eurofins Genomix Company (Ebersberg, Germany) (1).

Stereotaxic microinjection of lentiviral expression vectors

Lentiviral vectors expressing green fluorescent protein (GFP) and inhibiting SIRT1 (shSIRT1), FOXO1 (shFOXO1), MCHR1 (shMCHR1), POMC (shPOMC) ($3{,}1X10^{06}$ PFU/ml) (SIGMA-Aldrich) and GABA-R (shGABA-R) genes or scrambled sequences were injected bilaterally into the ARC (anterior to bregma (AP) −2.85 mm, lateral to the sagittal suture (L) ±0,3 mm, and ventral from the surface of the skull (V) -10,2 mm), with a microliter syringe (2; 3). The viral particles (1 μl, $3{,}1X10^{06}$ PFU/ml) were infused over 5 minutes and the injector kept in place for an additional 5 minutes. GFP fluorescence using a fluorescent visualized under the microscope was used as a visual marker of effective transduction of the lentivirus at the injection site. Dissection of the ARC was performed by micropunches under the microscope, as previously shown (4; 5).

Stereotaxic AAV-DREADD-mCherry injections

The hM3Dq coding sequences were cloned into a mCherry vector upstream of the mCherry sequence to generate C-terminal mCherry fusion proteins (Addgene, Cambridge, USA). The hM3Dq-mCherry coding sequence was amplified by PCR, and the amplicons and a cre-inducible AAV vector with a human *Synapsin 1* promoter was packaged in serotype 8: $7.53X10^{12}$ PFU/ml genome copies per mL and was prepared and tittered at the Universidad Autonoma de Barcelona (Barcelona, Spain). ketamine-xylazine anesthesized male *AgRP-Ires-cre* mice (6) were placed in a stereotaxic frame (David Kopf Instruments). The CRE-dependent AVV were injected bilaterally into the ARC of all mice (anterior to bregma (AP) −1.5 mm, lateral to the sagittal suture (L) ±0,2 mm, and ventral from the surface of the skull (V) -6 mm) with a microliter syringe (neuros model 7001 KH, Hamilton, USA). The viral particles (1 μl, $7.53X10^{09}$ PFU/ml) were infused over 10 minutes and the injector kept in place for an additional 5 minutes. Detection of mCherry was performed with an immunofluorescence procedure, using a rabbit anti-cherry (1:200; *Abcam*; Cambridge, UK). Detection was done with an anti-rabbit antibody conjugated with *Alexa 488* (1:200; *Molecular Probes;* Grand Island, NY, US)

Food intake experiments involving MCH-ASO or MCH-sense *in AgRP-Ires-cre* mice started after 30 min of CNO (1 mg/kg of body weight) or vehicle- i.p. injection. These mice were singly housed for at least 2 weeks beforehand.

Intracerebroventricular infusions

Rats and mice were anesthetized and cannulate to an osmotic minipump (model 2001 Alzet Osmotic Pumps; DURECT, CA) as previously described (2; 7). The minipump was inserted in subcutaneous

pocket on the dorsal surface. MCH was continuously infused in rats and mice at the following concentrations:10μg/day and 2.5μg/day respectively. The incision was closed with sutures, and rats were kept warm until full recovery.

Brain slice preparation

Hypothalamic slices were cut from 8- to 12-week-old male Pomc-Cre:ROSA-tdTomato mice as previously described (8). Briefly, mice were anaesthetized with isoflurane, and after decapitation, the brain was rapidly removed and put in ice-cold oxygenated (O_2 95% / CO_2 5%) artificial cerebrospinal fluid (ACSF) containing the following (in mM): 120 NaCl, 3.2 KCl, 1 NaH_2PO_4, 26 $NaHCO_3$, 1 $MgCl_2$, 2 $CaCl_2$, 2.5 glucose (osmolarity adjusted to 300 mOsm with sucrose, pH 7.4). After removal of the cerebellum, the brain was glued and coronal hypothalamic slices (250 μm thick) containing the ARC were cut using a vibratome (VT1200S; Leica). Before recording, slices were incubated at 35ºC for a recovery period of 1 h. After recovery, slices were placed in a submerged recording chamber (31ºC; Warner Instruments) and continuously perfused (2 ml/min) with oxygenated ACSF. Physiological concentration of glucose (2.5 mM) was used for recording (8). MCH was applied to the perfusing system (bath application) to obtain a final concentration of 1 μM.

Patch-clamp recordings

ARC POMC neurons expressing the fluorophore td-Tomato were visualized with a 40x objective in an upright video-microscope Leica DM-LFSA equipped with fluorescence and infrared differential interference contrast (IR-DIC). Whole-cell patch-clamp recordings were performed in current-clamp mode as previously described (8) by using a Multiclamp 700B amplifier (Molecular Devices). Data were filtered at 1 kHz and sampled at 5 kHz with Digidata 1322A interface and Clampex 10.6 from pClamp software (Molecular Devices). Pipettes (from borosilicate capillaries; World Precision Instruments) had a resistance of 6-8 MΩ when filled with an internal solution containing the following (in mM): 123 K-gluconate, 2 $MgCl_2$, 8 KCl, 0.2 EGTA, 4 Na_2-ATP, 0.3 Na-GTP, and 10 HEPES, pH 7.3 with KOH. Loose patch-clamp recordings were performed in current-clamp mode. All recordings were analyzed with Clampfit 10.6 from pClamp software (Molecular Devices). Junction potential was determined to allow correction of membrane potential values. A series of current pulses from – 60 to 70 pA (1 s, 10 pA increments) was applied to measure the passive membrane properties of ARC POMC neurons.
Mean firing rate values were obtained before, during, and after MCH treatment. Neurons were considered responsive when a change of more than 20% in firing rate was observed. The peak response was determined, and the number of spikes was counted 2 min before and after the peak effect. Basal and recovery firing rate values were obtained by counting the number of spikes during a 4-min period before and after treatment, respectively.

Glucose tolerance test

Glucose-tolerance tests (GTT) were performed by injection of glucose (2 mg/g) intraperitoneally (ip) after 6 h fasting. Blood samples were collected immediately before and 15, 30, 60 and 120 min after glucose administration (9; 10).

Sympathetic nerve activity (SNA) recording

Mice were anesthetized with ip ketamine (91 mg kg-1) and xylazine (9.1 mg kg-1). Anesthesia was maintained with α-chloralose (initial dose: 25mg kg-1, sustain dose: 50 mg kg-1 h-1) via a catheter inserted in the femoral vein. The trachea was cannulated, and each mouse was allowed to breathe

spontaneously oxygen-enriched air. Rectal temperature was maintained at 37.5°C using a temperature-controlled surgical table and a lamp. We obtained multi-fiber recording of SNA as previously described (2). Using a dissecting microscope, a nerve fiber innervating WAT was identified, placed on the bipolar platinum-iridium electrode. Each electrode was attached to a high-impedance probe (HIP-511, Grass Instruments) and the nerve signal was amplified 105 times with a Grass P5 AC pre-amplifier. After amplification, the nerve signal was filtered at a 100- and 1000-Hz cutoff with a nerve traffic analysis system (Model 706C, University of Iowa Bioengineering). The nerve signal was then routed to an oscilloscope (model 54501A, Hewlett-Packard) for monitoring the quality of the sympathetic nerve recording and to a resetting voltage integrator (model B600c, University of Iowa Bioengineering). SNA measurements were made every 15 min for 6 h after icv. To ensure that electrical noise was excluded in the assessment of sympathetic outflow, we corrected each SNA recording for post-mortem background activity.

Western blot analysis

Western blot were performed as previously described (2; 11-13). Hypothalami, ARC, MBH, WAT and liver protein lysates were homogenized in ice-cold lysis buffer containing 50 mmol/L Tris-HCl (pH 7.5), 1 mmol/L EGTA, 1 mmol/l EDTA, 1% Triton X-100, 1 mmol/l sodium orthovanadate, 50 mmol/l sodium fluoride, 5 mmol/l sodium pyrophosphate, 0.27 mol/l sucrose, 0.1% 2-mercaptoethanol, and complete protease and phosphatase inhibitor cocktail (1 tablet/50 ml; Roche Diagnostics, Mannheim, Germany). Homogenates were centrifuged at 13.000g for 10 min at 4°C, supernatants were removed, and aliquots were snap-frozen in liquid nitrogen. Hypothalamic and ARC protein lysates were subjected to SDS-PAGE on 8% and 12% polyacrylamide gels and electrotransferred on a polyvinylidene fluoride membrane. Briefly, total protein lysates from hypothalamus (40 μg) or ARC (20 μg) were subjected to SDS-PAGE, electrotransferred on a polyvinylidene difluoride membrane. Membranes were blocked for 1 h in TBS-Tween 20 (TBST: 50 mmol/L Tris- HCl (pH 7.5), 0.15 mol/L NaCl, and 0.1% Tween 20) containing 5% skimmed milk or 3% BSA and probed for 16 h at 4°C in TBST, 5% skimmed milk or 3% BSA with antibodies against ACC, phospho-ACC-Ser79 (pACC), AMPKα1 and AMPKα2 (Upstate); phospho-AMPK-Thr172 (pAMPK), pHSL Ser680, SAPK/JUNK Thr183/Tyr185, FOXO1, acetyl-p53 and p53 (Cell Signaling); AgRP (Abcam); POMC, NPY, CART, FAS(H-300), SIRT1, CIDE-A (N-19)R, acetyl-Foxo1, GABA-R and MCH pro-peptide (Santa Cruz Biotechnology), MCHR1 (Abnova) or mTOR, p-mTOR and β-actin (Sigma-Aldrich). Given that some processed peptides are short and are unlikely to be electrophoretically resolved in a blot of polyacrylamide gel we used antibodies detecting pre-propeptides for POMC, NPY and AgRP (for more information please see supplementary **Table S2**). Because some mature peptides are too short to be electrophoretically resolved in a blot of polyacrylamide gel, we used antibodies detecting pre-propeptides for POMC, NPY and AgRP (for more information please see supplementary **Table S2**). Membranes were then incubated with horseradish peroxidase-conjugated secondary antibodies (Dako Denmark, Glostrup, Denmark) followed by chemiluminescence (Pierce ECL Western Blotting Substrate, Thermo scientific, USA). Then, the membranes were exposed to X-ray film (Super RX, Fuji Medical X-Ray Film, Fujifilm, Japan) and developed with developer and fixing liquids (AGFA, Germany) under appropriate dark room conditions. Protein levels were normalized to β-actin for each sample.

Real-time PCR

Real-time PCR (*TaqMan®, Applied Biosystems*; Foster City, CA, USA; or *SYBR® Green, Roche Molecular Biochemicals,* Mannheim, Germany*,* for the hypothalamic nuclei samples) was performed using specific primers and probes **(Table S1)** as previously described (14). Values were expressed in relation to hypoxanthineguanine phosphoribosyl-transferase (HPRT) levels.

SUPPLEMENTARY DATA

Liver TG content

The extraction procedure for liver TG was adapted from methods described previously (2). Livers (aprox 200 mg) were homogenized for 2 min in ice-cold chloroform-methanol (2:1, vol/vol). TG were extracted during 5-h shaking at room temperature. For phase separation, H_2O MQ was added, samples were centrifuged, and the organic bottom layer was collected. The organic solvent was dried using a Speed Vac and dissolved in chloroform. TG (Randox Laboratories LTD, UK) content of each sample was measured in duplicate after evaporation of the organic solvent using an enzymatic method.

Hematoxylin/eosin staining and immunohistochemistry
WAT and BAT samples were fixed in 10% formalin buffer for 24 h, and then dehydrated and embedded in paraffin by a standard procedure. Sections of 3 μm were prepared with a microtome and stained using a standard Hematoxylin/Eosin Alcoholic (BioOptica) procedure according to the manufacturer's instructions. Alternative sections of paraffin were used for immunohistochemistry detection of UCP-1. Immunohistochemistry was performed as previously described (15; 16) using a rabbit anti-UCP-1 (1:500 for WAT and 1:2000 for BAT; Abcam; Cambridge, UK). UCP-1-positive cells were counted by using Image J.

Immunofluorescence

Mice brains were fixed by perfusion followed by immersion (12 h) in 10% buffered formalin for 24 hours. The brain pieces were cut 50 μm thick using a Vibratome® Series 1000. Detection of GFP, and POMC immunofluorescence; and double labelling were performed as previously reported (15; 17).

SUPPLEMENTARY DATA

Supplementary Figure 1. Protein expression of some molecular markers after central MCH administration in the ARC. Central effects of icv MCH administration (20µg/rat) on, **(A)** hypothalamic protein levels of FAS, ACC, pACC, AMPKα1, AMPKα2, pAMPK, mTOR and p-mTOR and **(B)** hypothalamic protein levels of NPY and CART in rats after 2 hours. β-actin was used to normalize protein levels. Dividing lines indicate spliced bands from the same gel. Values are mean ± SEM of 7–10 animals per group.

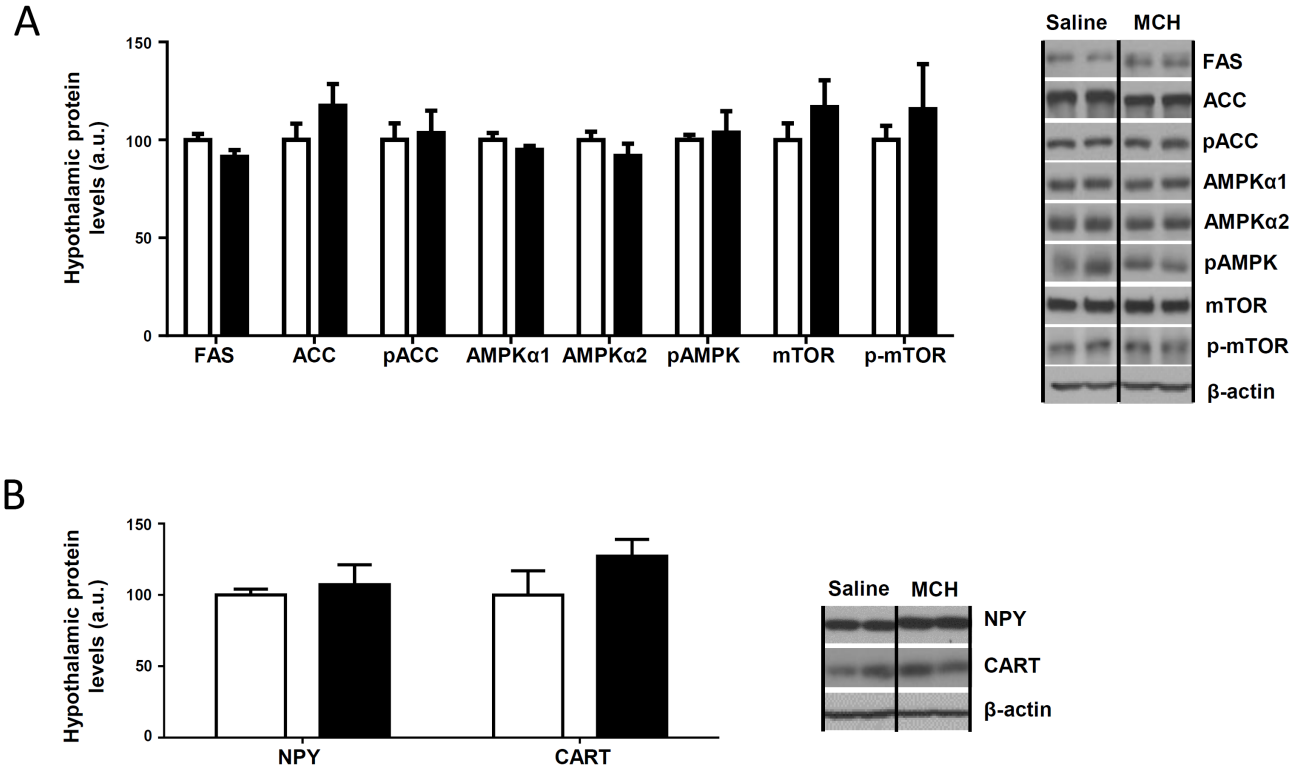

SUPPLEMENTARY DATA

Supplementary Figure 2. Intracellular pathway induced by MCH in the ARC and specificity of the nuclei isolation. mRNA levels of FOXO1 (A), POMC (B) and AgRP (C) in the ARC after icv injection of MCH. VMH FOXO1 mRNA (D) and LHA (E) FOXO1 mRNA expression after icv MCH injection. VMH SIRT1 and FOXO1 protein levels (F) and LHA SIRT1 and FOXO1 protein levels (G) after the injection of MCH directly in the ARC. mRNA levels of POMC (H) and SF-1 (I) were measured in the ARC and VMH. Values are mean ± SEM of 5–8 animals per group. *$P \leq 0.05$, **$P \leq 0.01$ and ***$P \leq 0.001$ *vs* controls.

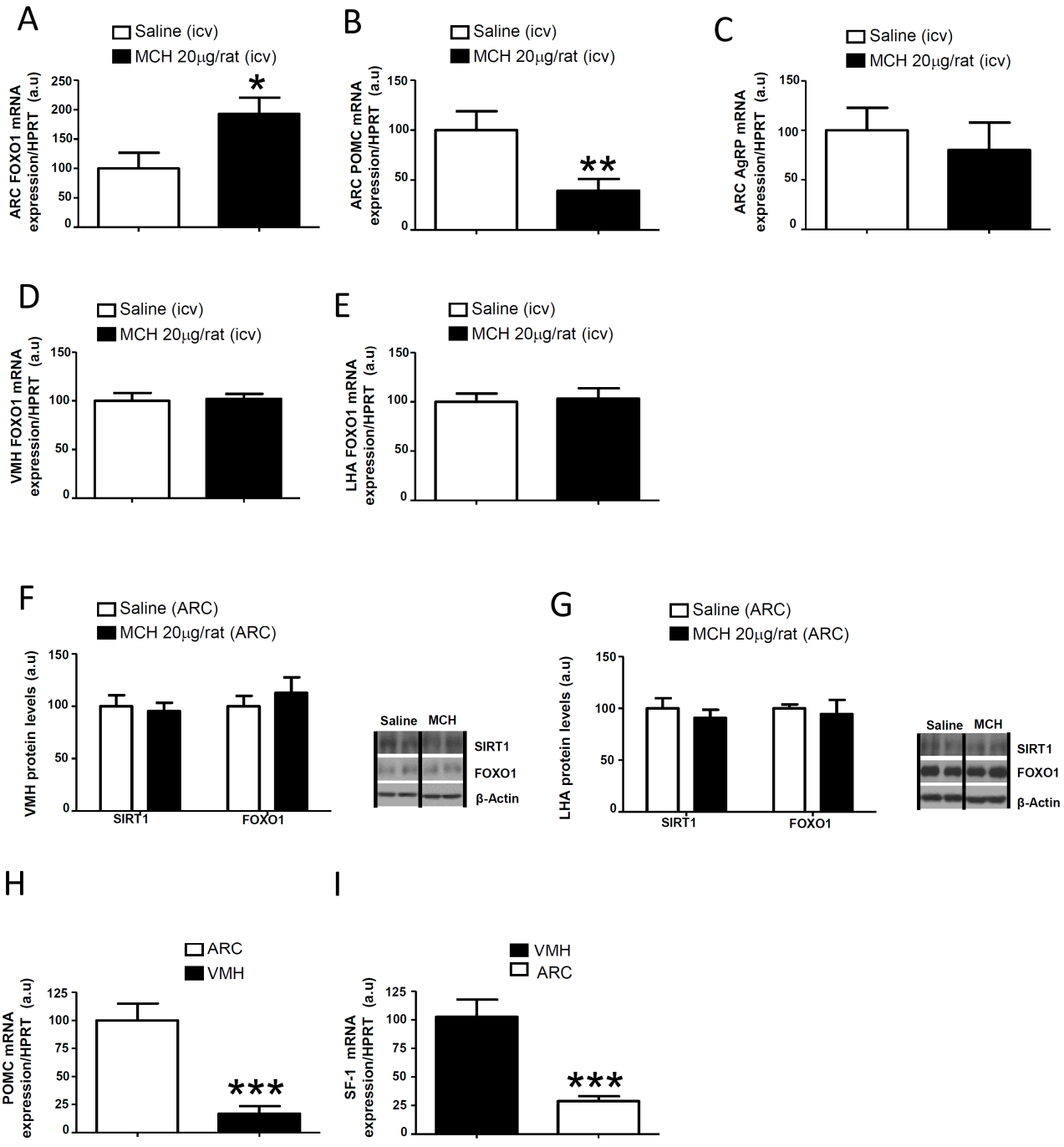

SUPPLEMENTARY DATA

Supplementary Figure 3. The MCH orexigenic action is blunted by the pharmacological blockade of SIRT1. Effects of icv injection of MCH (20µg/rat) and EX-527 (10µg/rat) + MCH (20µg/rat) compared to vehicle injected controls on food intake after 2h (A). Body weight change (B) and cummulative food intake (C) after 2 weeks of shSIRT1 injection or GFP scrambled lentiviruses into the ARC of rats before MCH administration. Values are mean ± SEM of 8–10 animals per group. **P*≤0.05, ***P*≤0.01; and ****P*≤0.001 *vs* controls.

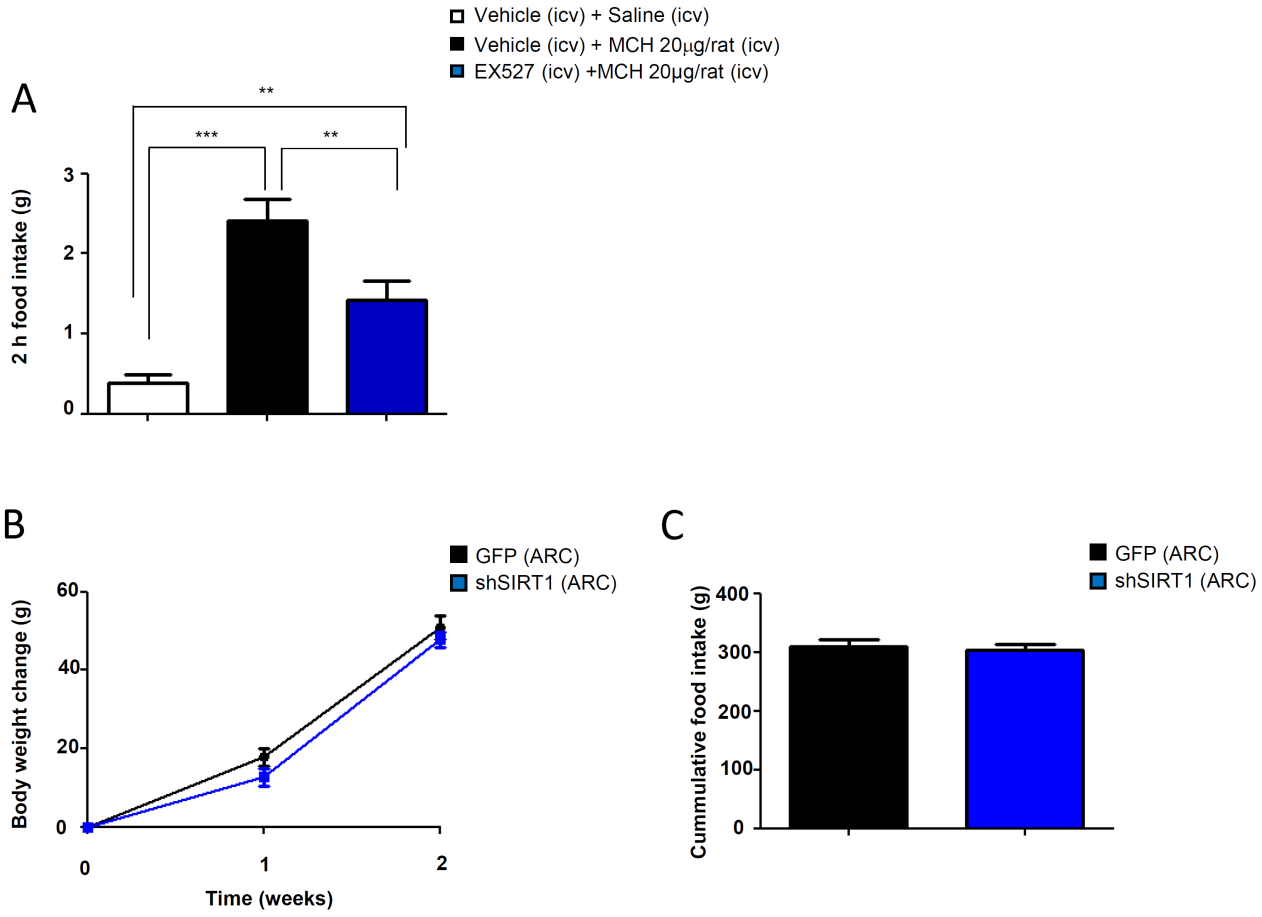

SUPPLEMENTARY DATA

Supplementary Figure 4. Central MCH requires SIRT1 and FoxO1 in the hypothalamic ARC to induces adiposity. Representative pictures of WAT and BAT histology (hematoxylin-eosin) and WAT and BAT protein levels of UCP1; Values are mean ± SEM of 5–10 animals per group.

SUPPLEMENTARY DATA

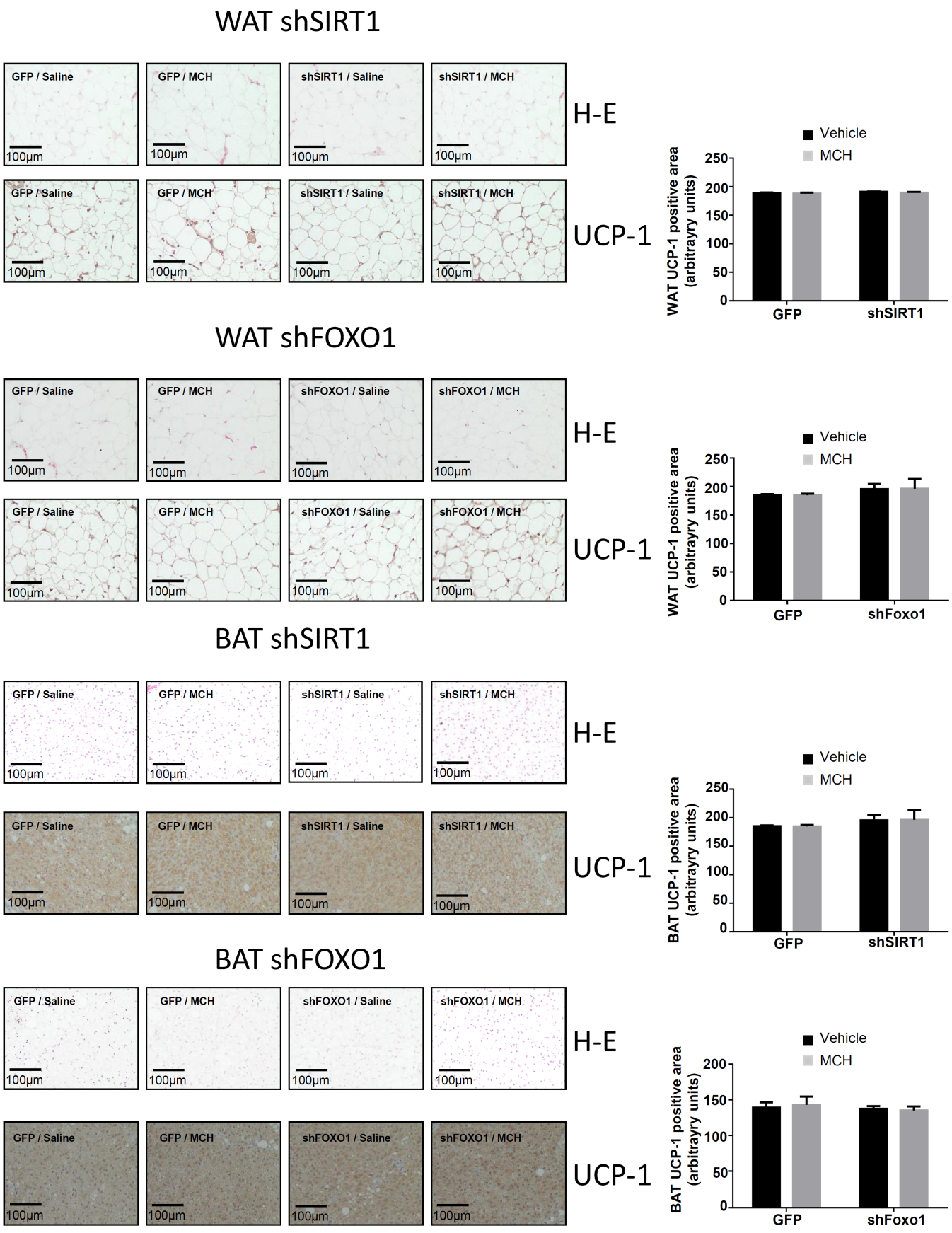

SUPPLEMENTARY DATA

Supplementary Figure 5. Central inhibition of MCH induces hypophagia. MCH protein levels in the different models evaluated with MCH-ASO: wild type mice (A) and SIRT1 Tg mice (B). Values are mean ± SEM of 5–10 animals per group. *$P \leq 0.05$, **$P \leq 0.01$; and ***$P \leq 0.001$ *vs* controls.

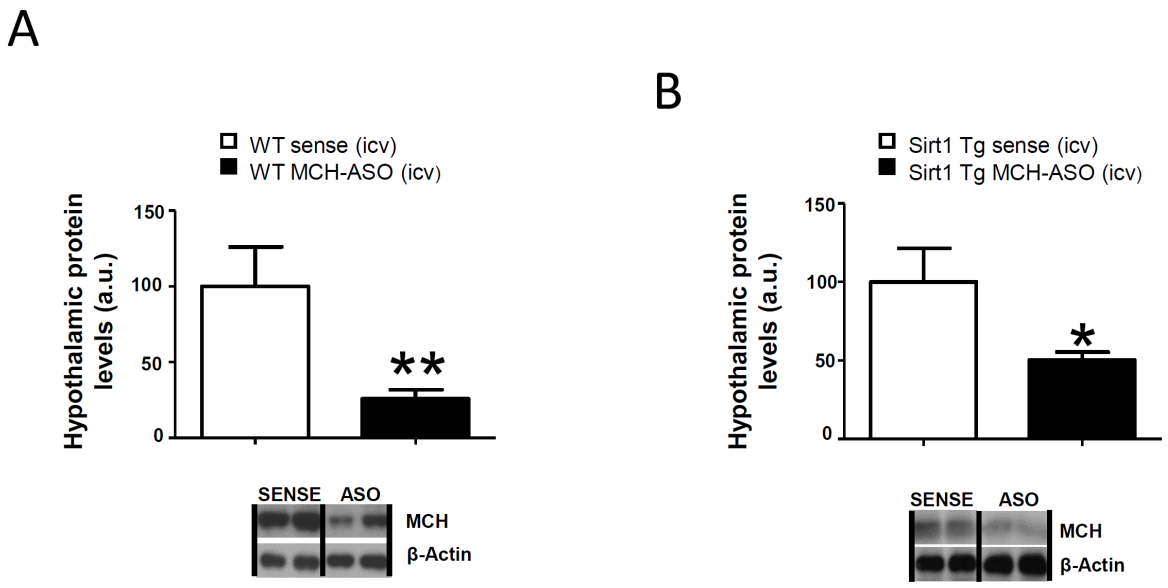

Appendix figures. Uncropped blots.

Supplementary Table 1 related to Figure S2: Primers and probes for real-time PCR (TaqMan®) analysis.

mRNA	Gene name	Gene bank accession number	Sequence of primers
AgRP	Agouti-related protein	NM 00360.1	FWD: 5'-CAG AGT TCT CAG GTC TAA GTC-3 REV: 5'-TTG AAG AAG CGG CAG TAG CAC-3'
Fox01	Forkhead box protein 01	NM 001191846.2	FWD: 5'-TGT GCC CTA CTT CAA GGA TAA GG-3' REV: 5'-GTG GCG AAT TGA ATT CTT CCA-3'
Hprt	Hypoxanthine Phosphoribosyltransferase-1	NM 012583	FWD: 5'-AGC CGA CCG GTT CTG TCA T-3' REV: 5'-GGT CAT AAC CTG GTT CAT CAT CAC-3'
POMC	Pro-opiomelanocortin	NM 139326.2	FWD: 5'-CGT CCT CAG AGA GCT GCC TTT-3' REV: 5'-TGT AGC AGA ATC TCG GCA TCT TC-3'
Sf-1	Steroidogenic factor-1		Assay ID Applied Biosystems TaqMan® Gene Expression Assays Assay ID Rn00584298_m1

SUPPLEMENTARY DATA

Protein	Name of Antibody	Manufacturer, catalog and lot #, and/or name of individual providing the antibody	Species raised in	Dilution used	Lot
ACC	Anti-ACC	Millipore, 04-322	rabbit	1:1000	Not available
Acetyl Foxo1	Anti-Acetyl-FKHR	Santa Cruz Biotechnology, sc-101681	rabbit	1:1000	DO915
Acetyl-p53	Anti-acetyl p53	Cell Signaling, #2570	rabbit	1:500	4
AgRP	Anti-AgRP propeptide	Abcam, ab113481	rabbit	1:1000	GR66371-6
AMPKα1	Anti-AMPKα1	Millipore #07-350	rabbit	1:1000	2684946
AMPKα2	Anti-AMPKα2	Millipore #07-363	rabbit	1:1000	2475668
β-actin	Anti-β-Actin	Sigma-Aldrich A 5316	mouse	1:10000	067M4781V
CART	Anti-CART (N20)	Santa Cruz Biotechnology, sc-18068	GOAT	1:1000	I1911
CIDE-A	Anti-CIDE-A (N-19)R	Santa Cruz Biotechnology, sc-8730-R	rabbit	1:1000	K1209
FAS	Anti-FAS (H-300)	Santa Cruz Biotechnology, sc-20140	rabbit	1:1000	G1813

Supplementary Table 2: List of antibodies used in the western blots and immunohistochemistry methods.

FOXO1	Anti-Fox01 (C29H4)	Cell Signaling, #2880	rabbit	1:1000	11
GABA-R	Anti-GABA-RAP (FL-117)	Santa Cruz Biotechnology sc-28938	rabbit	1:1000	J2708
GFP	Anti-GFP	Abcam, ab13970	chicken	1:4000	GR3190550-14
MCH	Anti-MCH pro-peptide	Santa Cruz Biotechnology sc-28931	rabbit	1:1000	B2006
MCHR1	Anti-MCH-R	Abnova PAB16225	rabbit	1:1000	5487/5488AP3-1
mTOR	Anti-mTOR	Cell Signaling, #2972	rabbit	1:1000	10
NPY	Anti-NPY propeptide	Sigma-Aldrich, WH0004852	mouse	1:1000	09121-3B5
pACC	Anti-phospho-ACC-Ser79	Cell Signaling, #3661	rabbit	1:1000	10
pAMPK	Anti-phospho-AMPK-Thr172	Cell Signaling, 2535	rabbit	1:1000	21
pHSL	Anti-phospho HSL (ser 680)	Cell Signaling, 4126	rabbit	1:1000	6
pJNK	Anti-SAPK/JUNK Thr183/Tyr185	Cell Signaling, #4668	rabbit	1:1000	11
p-mTOR	Anti-p-mTOR (Ser 2448)	Cell Signaling, #2971	rabbit	1:1000	21
POMC	Anti-POMC propeptide (FL-267)	Santa Cruz Biotechnology, sc-20148	rabbit	1:1000	G2810
POMC	Anti-POMC propeptide	Phoenix pharmaceuticals, H029-30	rabbit	1:200	01800-4
p53	Anti-p53 (1C12) mouse mAB	Cell Signalling, #2524S	mouse	1:1000	13
SIRT1	Anti-SIRT1 (H-300)	Santa Cruz Biotechnology, sc-15404	rabbit	1:1000	Not available

SUPPLEMENTARY DATA

Supplementary references

1. Pereira-da-Silva M, De Souza CT, Gasparetti AL, Saad MJ, Velloso LA: Melanin-concentrating hormone induces insulin resistance through a mechanism independent of body weight gain. J Endocrinol 2005;186:193-201
2. Imbernon M, Beiroa D, Vazquez MJ, Morgan DA, Veyrat-Durebex C, Porteiro B, Diaz-Arteaga A, Senra A, Busquets S, Velasquez DA, Al-Massadi O, Varela L, Gandara M, Lopez-Soriano FJ, Gallego R, Seoane LM, Argiles JM, Lopez M, Davis RJ, Sabio G, Rohner-Jeanrenaud F, Rahmouni K, Dieguez C, Nogueiras R: Central melanin-concentrating hormone influences liver and adipose metabolism via specific hypothalamic nuclei and efferent autonomic/JNK1 pathways. Gastroenterology 2013;144:636-649 e636
3. Aponte Y, Atasoy D, Sternson SM: AGRP neurons are sufficient to orchestrate feeding behavior rapidly and without training. Nature neuroscience 2011;14:351-355
4. Martinez de Morentin PB, Gonzalez-Garcia I, Martins L, Lage R, Fernandez-Mallo D, Martinez-Sanchez N, Ruiz-Pino F, Liu J, Morgan DA, Pinilla L, Gallego R, Saha AK, Kalsbeek A, Fliers E, Bisschop PH, Dieguez C, Nogueiras R, Rahmouni K, Tena-Sempere M, Lopez M: Estradiol regulates brown adipose tissue thermogenesis via hypothalamic AMPK. Cell Metab 2014;20:41-53
5. Imbernon M, Sanchez-Rebordelo E, Gallego R, Gandara M, Lear P, Lopez M, Dieguez C, Nogueiras R: Hypothalamic KLF4 mediates leptin's effects on food intake via AgRP. Mol Metab 2014;3:441-451
6. Koch M, Varela L, Kim JG, Kim JD, Hernandez-Nuno F, Simonds SE, Castorena CM, Vianna CR, Elmquist JK, Morozov YM, Rakic P, Bechmann I, Cowley MA, Szigeti-Buck K, Dietrich MO, Gao XB, Diano S, Horvath TL: Hypothalamic POMC neurons promote cannabinoid-induced feeding. Nature 2015;519:45-50
7. Gomori A, Ishihara A, Ito M, Mashiko S, Matsushita H, Yumoto M, Tanaka T, Tokita S, Moriya M, Iwaasa H, Kanatani A: Chronic intracerebroventricular infusion of MCH causes obesity in mice. Melanin-concentrating hormone. Am J Physiol Endocrinol Metab 2003;284:E583-588
8. Clasadonte J, Scemes E, Wang Z, Boison D, Haydon PG: Connexin 43-Mediated Astroglial Metabolic Networks Contribute to the Regulation of the Sleep-Wake Cycle. Neuron 2017;95:1365-1380 e1365
9. Perez-Sieira S, Martinez G, Porteiro B, Lopez M, Vidal A, Nogueiras R, Dieguez C: Female Nur77-deficient mice show increased susceptibility to diet-induced obesity. PloS one 2013;8:e53836
10. Contreras C, Gonzalez-Garcia I, Martinez-Sanchez N, Seoane-Collazo P, Jacas J, Morgan DA, Serra D, Gallego R, Gonzalez F, Casals N, Nogueiras R, Rahmouni K, Dieguez C, Lopez M: Central ceramide-induced hypothalamic lipotoxicity and ER stress regulate energy balance. Cell reports 2014;9:366-377
11. Beiroa D, Imbernon M, Gallego R, Senra A, Herranz D, Villarroya F, Serrano M, Ferno J, Salvador J, Escalada J, Dieguez C, Lopez M, Fruhbeck G, Nogueiras R: GLP-1 Agonism Stimulates Brown Adipose Tissue Thermogenesis and Browning Through Hypothalamic AMPK. Diabetes 2014;63:3346-3358
12. Lopez M, Lage R, Saha AK, Perez-Tilve D, Vazquez MJ, Varela L, Sangiao-Alvarellos S, Tovar S, Raghay K, Rodriguez-Cuenca S, Deoliveira RM, Castaneda T, Datta R, Dong JZ, Culler M, Sleeman MW, Alvarez CV, Gallego R, Lelliott CJ, Carling D, Tschop MH, Dieguez C, Vidal-Puig A: Hypothalamic fatty acid metabolism mediates the orexigenic action of ghrelin. Cell Metab 2008;7:389-399
13. Lopez M, Varela L, Vazquez MJ, Rodriguez-Cuenca S, Gonzalez CR, Velagapudi VR, Morgan DA, Schoenmakers E, Agassandian K, Lage R, Martinez de Morentin PB, Tovar S, Nogueiras R, Carling D, Lelliott C, Gallego R, Oresic M, Chatterjee K, Saha AK, Rahmouni K, Dieguez C, Vidal-Puig A:

SUPPLEMENTARY DATA

Hypothalamic AMPK and fatty acid metabolism mediate thyroid regulation of energy balance. Nature medicine 2010;16:1001-1008
14. Zhan C, Zhou J, Feng Q, Zhang JE, Lin S, Bao J, Wu P, Luo M: Acute and long-term suppression of feeding behavior by POMC neurons in the brainstem and hypothalamus, respectively. The Journal of neuroscience : the official journal of the Society for Neuroscience 2013;33:3624-3632
15. Quinones M, Al-Massadi O, Folgueira C, Bremser S, Gallego R, Torres-Leal L, Haddad-Tovolli R, Garcia-Caceres C, Hernandez-Bautista R, Lam BYH, Beiroa D, Sanchez-Rebordelo E, Senra A, Malagon JA, Valerio P, Fondevila MF, Ferno J, Malagon MM, Contreras R, Pfluger P, Bruning JC, Yeo G, Tschop M, Dieguez C, Lopez M, Claret M, Kloppenburg P, Sabio G, Nogueiras R: p53 in AgRP neurons is required for protection against diet-induced obesity via JNK1. Nat Commun 2018;9:3432
16. Al-Massadi O, Porteiro B, Kuhlow D, Kohler M, Gonzalez-Rellan MJ, Garcia-Lavandeira M, Diaz-Rodriguez E, Quinones M, Senra A, Alvarez CV, Lopez M, Dieguez C, Schulz TJ, Nogueiras R: Pharmacological and Genetic Manipulation of p53 in Brown Fat at Adult But Not Embryonic Stages Regulates Thermogenesis and Body Weight in Male Mice. Endocrinology 2016;157:2735-2749
17. Quinones M, Al-Massadi O, Gallego R, Ferno J, Dieguez C, Lopez M, Nogueiras R: Hypothalamic CaMKKbeta mediates glucagon anorectic effect and its diet-induced resistance. Mol Metab 2015;4:961-970